Available online at www.sciencedirect.com

ScienceDirect

ELSEVIER

Polymer 48 (2007) 590–597

polymer

www.elsevier.com/locate/polymer

Blends of poly(2,6-dimethyl-1,4-phenylene oxide) (PPO) with polystyrene-based thermoplastic rubbers: A comparative study

Judit E. Puskas [a,*], Yongmoon Kwon [a,b], Volker Altstädt [c], Marianna Kontopoulou [d]

[a] *Department of Polymer Science, The University of Akron, Goodyear Polymer Center, Room 420, 170 University Avenue, Akron, OH 44325-3909, USA*
[b] *Department of Chemical and Biochemical Engineering, University of Western Ontario, London, ON N6A 5B9, Canada*
[c] *Department of Polymer Engineering, University of Bayreuth, Universitätstr. 30, D-95440 Bayreuth, Germany*
[d] *Department of Chemical Engineering, Queen's University, Kingston, ON K7L 3N6, Canada*

Received 28 September 2006; received in revised form 21 November 2006; accepted 22 November 2006
Available online 15 December 2006

Abstract

This work presents the first part of our study on the modification of poly(2,6-dimethyl-1,4-phenylene oxide) (PPO) with styrenic thermoplastic rubbers. Polystyrene-*b*-polyisobutylene-*b*-polystyrene (SIBS), polystyrene-*b*-polybutadiene-*b*-polystyrene (SBS) and polystyrene-*b*-poly(ethylene/butylene)-*b*-polystyrene (SEBS) triblock copolymers were melt blended with PPO and the blends were characterized. Differential scanning calorimetry (DSC), dynamic mechanical thermal analysis (DMTA) and transmission electron microscopic (TEM) studies revealed that PPO/SEBS blends displayed the most pronounced phase-separated morphology with largest rubbery domains. SBS showed the most miscibility, and the least detrimental effect on dynamic mechanical properties and tensile strength. The results of this comparative study guided us to develop optimum conditions for the impact modification of PPO by SIBS thermoplastic rubbers.

Keywords: Polymer blend; Poly(2,6-dimethyl-1,4-phenylene oxide); Styrenic thermoplastic rubbers (SIBS, SEBS, SBS)

---

1. Introduction

PPO (or PPE) (Poly(2,6-dimethyl-1,4-phenylene oxide or ether)) is a very attractive material due to its high strength, high heat distortion temperature, chemical resistance, stiffness, and fracture toughness [1,2]. However, its brittleness and poor processability have limited its industrial use in a wider range of applications [2]. In order to achieve desired mechanical properties PPO has been blended with various materials [2–10]. Since PPO and polystyrene (PSt) are completely miscible at all molecular weights and concentration ranges [3,4], PSt or its derivatives, such as high-impact PSt (HIPS, or polybutadiene-grafted polystyrene resin) and PSt-based block copolymers, have been used to improve the processability and toughness of pure PPO [5]. A good example is Noryl® by General Electric, an important engineering plastic produced by blending PPO with HIPS. Styrenic thermoplastic rubbers, such as polystyrene-*b*-polybutadiene-*b*-polystyrene (SBS) and its hydrogenated version, polystyrene-*b*-poly(ethylene/butylene)-*b*-polystyrene) (SEBS), and polystyrene-*b*-polyisobutylene-*b*-polystyrene (SIBS) have also been blended with PPO [2–4,6–10]. This latter is a relatively new type of thermoplastic rubber, which has become available commercially [11]. SIBS is chemically similar to SEBS in a sense that it has saturated elastomeric midblocks, and it demonstrates excellent chemical, oxidative and environmental stability [12]. Fig. 1 compares the chemical structures of the various thermoplastic rubbers. These materials exhibit thermoplastic elastomeric behavior, combining the good processability of thermoplastics with rubber elasticity. Ideally, the elastomer phase of the block copolymer should possess a solubility parameter sufficiently different from that of the PPO matrix to ensure fine phase dispersion, but the plastic phase should be compatible with PPO to ensure adequate adhesion of the elastomer phase to the matrix

---

[*] Corresponding author. Tel.: +1 330 972 6203; fax: +1 330 972 5290.
E-mail address: jpuskas@uakron.edu (J.E. Puskas).

0032-3861/$ - see front matter © 2006 Elsevier Ltd. All rights reserved.
doi:10.1016/j.polymer.2006.11.045

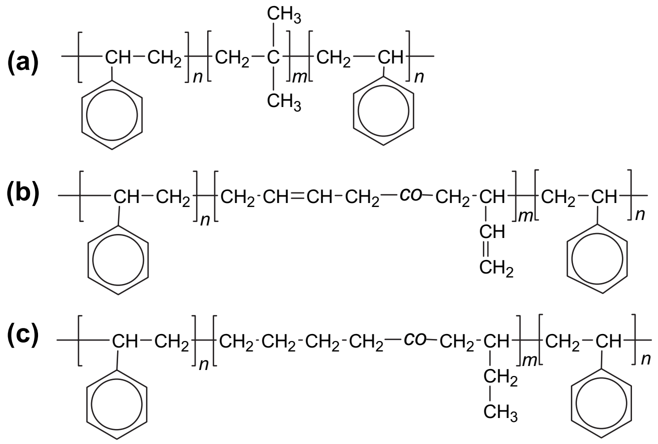

Fig. 1. Chemical structure of various thermoplastic elastomers: (a) SIBS, (b) SBS and (c) SEBS.

[13]. It has been shown that even though PPO is completely miscible with PSt, the elastomeric blocks in the thermoplastic rubber may prevent free dispersion of the PSt blocks within the PPO matrix. Tucker et al. reported that PPO is completely miscible with SBS, while immiscible with SEBS having relatively short PSt arms ($M_n < 14{,}000$ g/mol) [3,6]. The authors found no effect of the molecular weight of PPO on miscibility in the $M_n \sim 15{,}000–30{,}000$ g/mol range. Chiu and Hwung reported that the miscibility of the blends decreased with increasing elastomer segment's molecular weight [7]. Asthana and Kennedy demonstrated that PPO/star-branched SIBS prepared by solution blending [10] had good miscibility when low MW PPO ($M_n = 3100$ g/mol) was used, but were only partially miscible with higher MW PPO ($M_n = 10{,}500$ g/mol).

Given the interest in using thermoplastic rubbers for toughening of PPO, this work reports our first results concerning the thermal, mechanical and morphological properties of PPO/SIBS blends prepared by melt compounding, in comparison with PPO/SBS and PPO/SEBS blends.

2. Experimental

2.1. Materials

PPO ($M_n = 24{,}000$ g/mol, $M_w/M_n = 1.5$) without any PSt addition was provided by BASF AG. SIBS triblock copolymers (SIBS 103T, $M_n = 78{,}310$ g/mol, MWD = 1.74, 34 wt% PSt, and SIBS 073T, $M_n = 66{,}720$ g/mol, $M_w/M_n = 1.24$, 31 wt% PSt) were provided by Kaneka Co, Japan. Shell kindly provided SEBS (Kraton G1650, $M_n = 80{,}890$ g/mol, MWD = 1.01, 29 wt% PSt) and SBS (Kraton D1153, $M_n = 86{,}000$ g/mol, MWD = 1.01, 30 wt% PSt).

The molecular weight (MW) and molecular weight distribution (MWD) of the block copolymers were determined by SEC using a Waters system equipped with six Styragel-HR columns (10^6, 10^5, 10^4, 10^3, 500, and 100 Å pore sizes), thermostated at 35 °C, a Waters 410 DRI detector thermostated at 40 °C, a Dawn DSP 18 angle Laser Light Scattering (MALLS) detector (Wyatt Technology), and a Waters 996 UV detector. THF was used as a mobile phase at 1 ml/min, continuously distilled from CaH_2 and recirculated. The Astra software (version 4.73) controlled the acquisition of data from the detectors and processed the data to obtain MWs. The MW of SBS and SEBS was measured by using the 100% mass recovery method; the MW of SIBSs was measured by both known dn/dc (copolymer dn/dc was calculated based on the weight fraction and dn/dc of the individual components, PIB = 0.093, PSt = 0.183) and 100% mass recovery on the SEC columns. The PSt content of the SIBS blocks was measured by ^{1}H NMR using a Varian Gemini 400 MHz and deuterated-chloroform (d-$CDCl_3$) solvent. Material properties are summarized in Table 1; the values agree well with the nominal values provided by the manufacturers.

2.2. Blend and test specimen preparation

PPO/block copolymer blends with compositions of 95/5, 90/10, 80/20 (w/w) were prepared using a Brabender Plasticorder mixer (DSE 20/40) at a rotor-speed of 50 rpm. The temperature of the mixer was 240 °C, well above the glass transition temperature (T_g) of PPO (216.6 °C). Nitrogen gas was introduced during mixing to minimize oxidative degradation of the PPO or block copolymers. PPO was first added to the mixer slowly and was allowed to soften. Shortly thereafter, the block copolymer was added and mixed for 4 min. All blends were pulverized into small particles (the diameter of particles was less than 0.5 mm) and dried at 100 °C for more than 2 h before compression molding. The blends were compression molded into sheets at 280 °C for 20 min in an electrically heated hydraulic press at a pressure of 40 kN (10 min preheating without pressure, and then 10 min with 40 kN pressure). After compression molding, the plates were transferred to a water-cooled press where they were held at 80 kN for 30 min.

2.3. Differential scanning calorimetry (DSC)

Samples of 5–10 mg were placed into aluminum sample pans and sealed for testing in a METTLER TOLEDO DSC821. The heating rate was 20 °C/min, and the data were collected from the second and third scans. Glass transition temperatures (T_gs) were taken as the mean value between the onset and end point temperatures. Nitrogen atmosphere was used to minimize thermal degradation of the blends.

Table 1
Characterization of thermoplastic rubbers

Sample ID	M_n (g/mol)	M_w/M_n	PSt (wt%)	M_n PSt block (g/mol)	M_n elastomer (g/mol)	M_c (g/mol)
SIBS103T	78,300	1.74	34.2	13,400	51,500	9610
SIBS073T	66,700	1.24	31.0	10,300	46,100	9610
SEBS	80,900	1.01	29.0	11,600	57,700	1530
SBS	86,500	1.01	30.0	12,900	60,700	2150

2.4. Dynamic mechanical thermal analysis (DMTA)

Dynamic mechanical thermal analysis was performed on a Rheometrics Scientific RDA III in the temperature sweep mode at a frequency of 1 Hz with a heating rate of 4 °C/min. The shear storage and loss moduli (G' and G'') were measured using a free oscillating torsional pendulum within the linear viscoelastic region (0.1% strain). The RSIOrche600 software was used to analyze the results.

2.5. Tensile and charpy impact measurements

A Zwick Z020 was used to measure the tensile properties of S2 specimens according to ISO 527 at room temperature (23 °C). The crosshead speed was set initially to 1 mm/min up to 0.25% elongation in order to get accurate moduli values and was afterwards raised to 5 mm/min. For each blend, five specimens were tested and the average value is reported. The Xpert software was used to evaluate the data.

Charpy impact measurements were performed according to ISO 179eA using a Zwick 5113 machine. The work of the hammer was 50 J. Samples were notched prior to the impact test.

2.6. Transmission electron microscopy (TEM)

Ultra-thin sections (50 nm) were cut from compression molded specimens at room temperature with a Reichert Ultramicrotome FC4 equipped with a diamond knife. Ultra-thin sections were placed on gold grids and were stained by exposure to RuO_4 vapor for 1 h at room temperature. Transmission electron micrographs were taken on a LEO 922 TEM at an accelerating voltage of 200 kV.

2.7. Rheological characterization

Measurements of viscoelastic properties in the linear region were performed using a controlled stress rheometer (Viscotech by Reologica) in the oscillatory mode, with parallel plate fixtures (20 mm in diameter). The complex viscosities, η^*, and the dynamic storage and loss moduli (G' and G'') were measured as functions of frequency ω at 240 °C. All measurements were carried out under nitrogen atmosphere to limit degradation or absorption of moisture.

Temperature sweeps in the range of 180–300 °C were performed to detect whether an order–disorder transition temperature (ODT) exists for the block copolymers.

3. Results and discussion

3.1. Thermal properties

Blends of PPO with styrene-based block copolymers essentially consist of three phases: a soft elastomeric phase, with a glass transition at sub-ambient temperatures (~ -70 °C), a hard PSt phase ($T_g \sim 100$ °C) and a hard PPO phase ($T_g \sim 216.6$ °C). Due to the small fraction of the rubber phase, the sub-ambient transition could not be measured reliably. The location of the glass transition temperatures of the hard PPO and PSt phases in the blends can reveal whether there is some degree of intermixing at the molecular level.

The DSC thermograms of PPO-rich blends in this work showed a single hard-phase transition, corresponding to the PPO phase, whereas there was no detectable T_g for the PSt phase, presumably due to the low PSt content. Table 2 summarizes the midpoint T_g values and the differences between the end point and onset temperature for all PPO/block copolymer blends at various blend compositions. The T_g values corresponding to the PPO phase decreased significantly with increasing block copolymer component in PPO/SBS blends. The PPO/SIBS 103T and PPO/SIBS 073T blends showed minor to moderate decrease, while the PPO T_g of the PPO/SEBS blends remained virtually unchanged.

These results can be better illustrated in Fig. 2, which summarizes T_gs as a function of PPO content in the hard phase. Since shifts in T_g generally imply a higher degree of intermixing of the two phases, it can be concluded that the degree of PSt incorporation is higher in the PPO/SBS blends, compared to the other block copolymers. Limited incorporation of PSt into PPO may also be present in the PPO/SIBS 103T blends, given the very slight shifts observed. Information on the degree of intermixing between phases can also be obtained by comparing the breadth of the glass transition, ΔT_g, which represents the difference between the end point and onset temperatures (Table 2). The breadth of ΔT_g is associated with the intimacy of aggregation of the PSt and PPO in miscible blends [14]; broad transition suggests the presence of concentration gradients in the mixed hard phase [3,15]. The broader ΔT_g values of PPO/SIBS 103T blends when compared to those

Table 2
Glass transition behavior of PPO/block copolymer blends measured by DSC

PPO/TPE	Compositions											
	PPO/SIBS 103T			PPO/SIBS 073T			PPO/SEBS			PPO/SBS		
	Onset (°C)	Midpoint (°C)	ΔT_g (°C)	Onset (°C)	Midpoint (°C)	ΔT_g (°C)	Onset (°C)	Midpoint (°C)	ΔT_g (°C)	Onset (°C)	Midpoint (°C)	ΔT_g (°C)
100/0	212.9	216.6	7.4	212.9	216.6	7.4	212.9	216.6	7.4	212.9	216.6	7.4
95/5	212.6	216.6	8.0	211.6	215.6	8.0	212.8	216.6	7.6	203.9	207.9	8.0
90/10	206.7	213.4	13.4	212.6	215.9	6.6	212.4	216.7	8.6	199.5	204.8	10.6
80/20	204.6	211.5	13.8	208.3	213.3	10.0	211.7	215.5	7.6	188.3	197.2	17.8

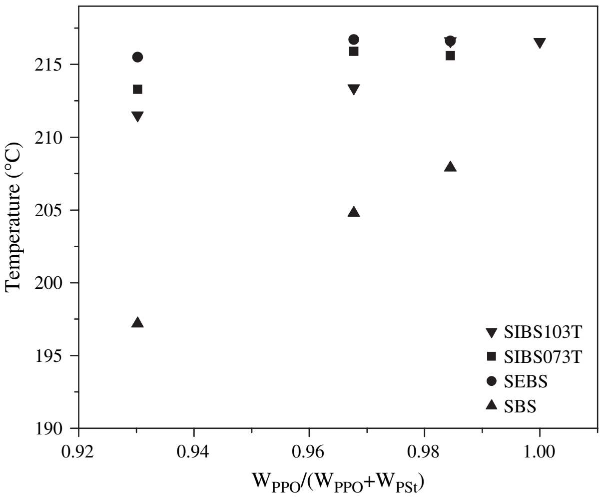

Fig. 2. Glass transition behavior of PPO modified with block copolymers determined by DSC. Composition is expressed as mass fraction of PPO, excluding the soft midblock.

Table 3
Solubility parameters of blend components

Sample	δ (cal/cm^3)$^{1/2}$
PPO	9.6 [16]
PSt	8.98 [17]
PIB	7.85 [17]
P(EB)	8.09 [17]
PB	8.18 [17]

of the PPO/SIBS 073T represent longer range concentration gradients in the PPO/PSt mixed phase. The MW of the PSt segments plays an important role in the miscibility of PPO and the PSt phase of the block copolymers; reportedly, higher PSt MW improves the miscibility with PPO [3,6,10]. Thus the greater depression of T_g values in the PPO/SIBS 103T blends might be due to the higher MW of the PSt segments of the SIBS 103T and/or the higher PSt content of SIBS 103T (see Table 1). The PPO/SBS blends have very broad ΔT_g values, indicating significant concentration gradients in the mixed hard domains. However, there is no observable change in the ΔT_g of the PPO/SEBS when compared to the ΔT_g of pure PPO, indicating the absence of or minimal intermixing between the two hard phases. This trend is somewhat surprising; in light of the solubility parameters shown in Table 3, less intermixing would be expected with SIBS than with SEBS, because of smaller solubility parameter difference between the rubber phase of the latter and PPO.

To get better insight into the blend morphology and its effect on mechanical properties, the phase morphologies of the blends were investigated by transmission electron microscopy (TEM) as discussed in Section 3.2.

3.2. Transmission electron microscopic analysis

Observation of the blends by TEM was facilitated by staining the materials with RuO_4. Both PPO and PSt can be stained with RuO_4, however, the rate of staining is very different. PSt domains stain faster [18], thus appearing as black regions in the photomicrographs.

Figs. 3 and 4 show the TEM micrographs of PPO/SIBS blends at various compositions. At very low dispersed phase contents (Figs. 3(a) and 4(a)), the block copolymer domains are well dispersed in the continuous PPO phase. A core–shell morphology can be seen, consisting of light-colored PIB phases at the center, surrounded by a PSt-rich phase (dark circles). The PIB domain size is between 20 and 40 nm.

Coalescence of the block copolymer phases can be observed with increasing SIBS block copolymer content (Figs. 3(b) and 4(b)), and co-continuous ‘‘lace-like’’ morphologies were obtained at 20 wt% SIBS content (Figs. 3(c) and 4(c)).

The morphology of PPO/SEBS appears to be coarser (Fig. 5a), with domain sizes of at least 100 nm. It is well known that two factors favoring a fine dispersion of the dispersed domains are viscosity ratio close to unity and low interfacial tension [19,20]. Rheological data (to be discussed in detail in Section 3.3) revealed that the viscosity ratio of PPO and SEBS is closer to unity than that of PPO and SIBS, thus higher interfacial tension between PPO and SEBS may be a possible reason for the appearance of a coarser morphology in PPO/SEBS blends.

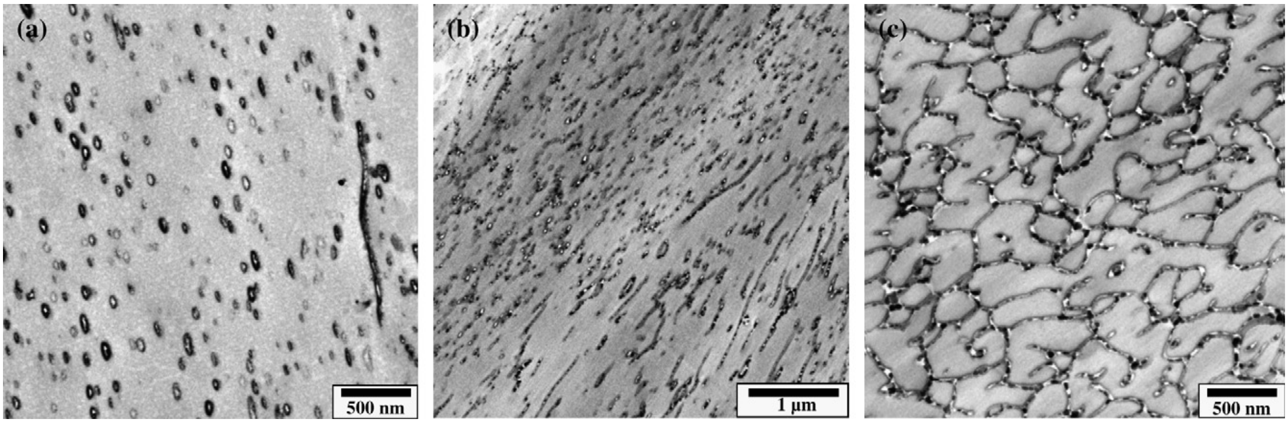

Fig. 3. TEM micrographs for PPO/SIBS (103T) blends (w/w): (a) 95/5, (b) 90/10, and (c) 80/20.

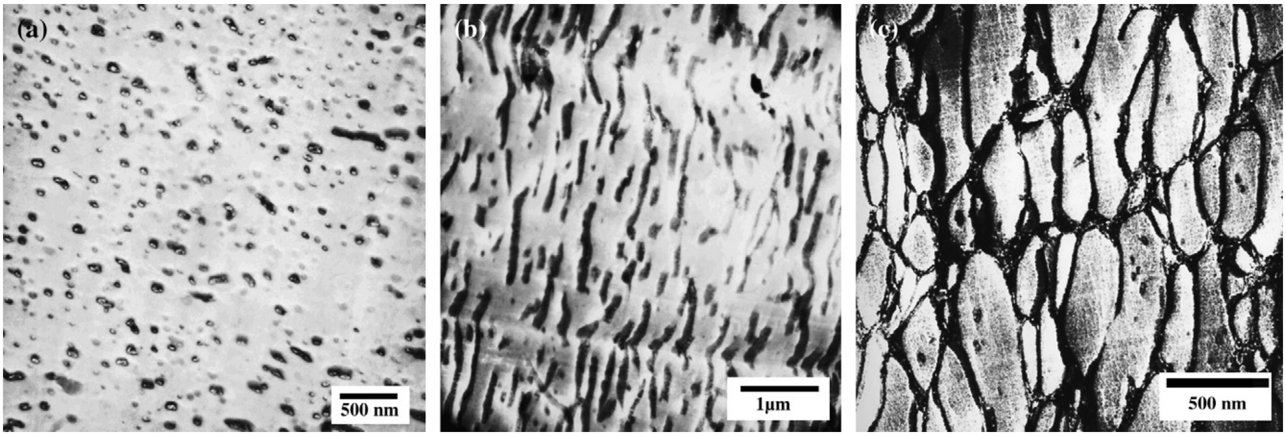

Fig. 4. TEM micrographs for PPO/SIBS (073T) blends (w/w): (a) 95/5, (b) 90/10, and (c) 80/20.

The micrographs of PPO/SBS blends represented in Fig. 6 are distinctly different from those of the previous blends, showing diffuse interphases and no discernable PSt phase (which would have a dark appearance due to staining). Due to smaller differences in solubility parameters in SBS block copolymers, the PSt and rubbery components have weaker repulsion between segments, causing an increase in interphase volume and increased mixing; thus the interphase in these block copolymers may appear diffuse, without the core–shell morphology seen in SEBS and SIBS. According to Tucker and others [4,6], the PSt segments of the SBS block copolymer are at least partially miscible with the PPO phase, resulting in better incorporation of the block copolymer into the PPO matrix.

Based on thermal analysis and TEM images, it is apparent that PSt segment incorporation into PPO is hindered when SEBS and SIBS block copolymers are used. Larger differences in solubility parameters may be a possible reason. The fact that compounding was carried out at 240 °C, well above the order–disorder transition (ODT) temperature of SBS (175–180 °C) [21], may have facilitated the incorporation of the PSt blocks into the PPO matrix, since at this temperature microphase separation no longer exists. On the contrary, temperature sweeps performed for the SIBS and SEBS block copolymers used in the current work did not reveal an ODT even at temperatures as high as 280 °C. In agreement with our results, Tse et al. did not detect a distinct discontinuity in viscosity at temperatures up to 300 °C for an SEBS with $M_n = 120,000$ g/mol containing 28 wt% PSt, indicating that the ODT for SEBS is probably near or higher than 300 °C [22]. It is thus suggested that the existence of microphase separation in the molten phase, with PSt blocks acting as physical crosslinks between the rubbery segments, may have hindered the incorporation of PSt into the PPO matrix at the compounding temperature of 240 °C. It should be noted that compounding at higher temperatures was not attempted, because of concern for excessive degradation of PPO. Solution blending of SIBS with lower MW PPO (80% PPO, $M_n = 10,500$ g/mol) led to better intermixing [10]. This blend displayed two distinct T_gs at around 150 and 200 °C, with a very broad transition in-between, suggesting the existence of two mixed (PSt-rich and PPO-rich) phases.

3.3. Rheological properties

The persistence of microphase separation in the SIBS and SEBS copolymers in the melt-state is evident from their rheological properties, showing the absence of a Newtonian plateau (Fig. 7a) and substantial deviations from terminal flow

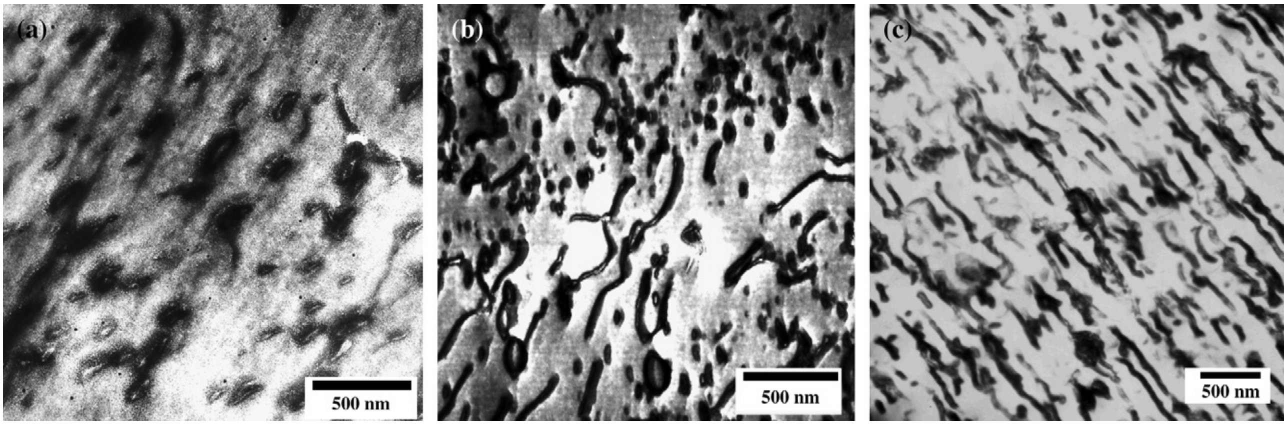

Fig. 5. TEM micrographs for PPO/SEBS blends (w/w): (a) 95/5, (b) 90/10, and (c) 80/20.

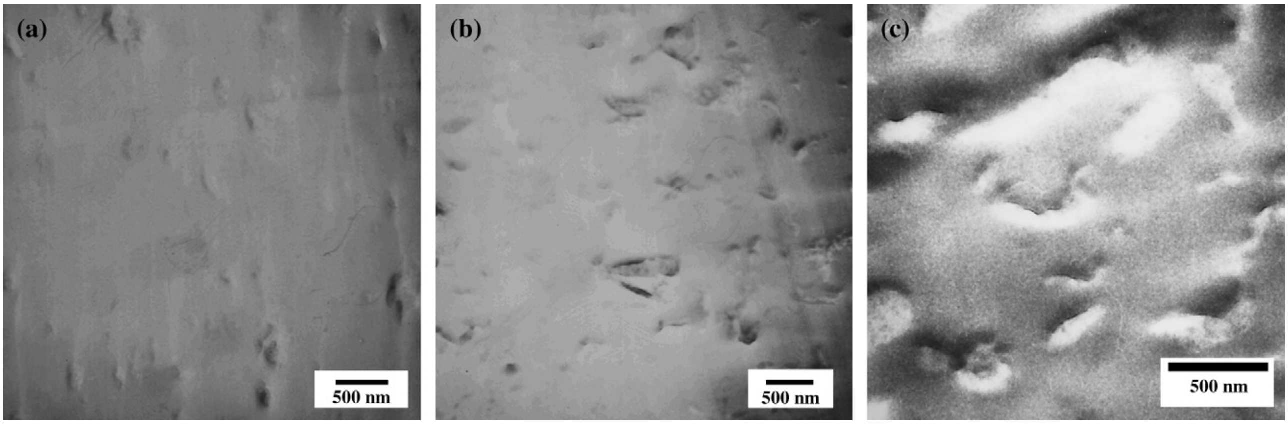

Fig. 6. TEM micrographs for PPO/SBS blends (w/w): (a) 95/5, (b) 90/10, and (c) 80/20.

behavior (Fig. 7b). Similar viscosity profile was reported for star-branched SIBS [10]. By contrast, it has been widely reported that SBS at temperatures above the ODT displays a Newtonian plateau [23].

It is worth noting that the two SIBS resins have very similar rheological properties, with SIBS 103T actually having slightly lower complex viscosity at high frequencies, and lower elastic modulus than SIBS 073T, in spite of its higher molecular weight. This may be due to the higher polydispersity of SIBS 103T, and/or a branched structure, leading to a more enhanced shear thinning character. The broad and multimodal molecular weight distribution of SIBS 103T is a strong indication of branching by PSt–PSt block coupling, an expected side reaction also seen in another commercial SIBS [24]. In addition, the lower PIB molecular weight in the SIBS 073T translates to a less elastic character in the melt (Fig. 7b). SEBS displays substantially higher viscosity and elasticity, in spite of its similar molecular weight and PSt block content, implying higher levels of entanglements than the rest of the block copolymers (see also Table 1). This is in line with the order of critical entanglement molecular weights of the elastomer blocks listed in Table 1. This suggests that SIBS should have 3–4 times higher elastomer block molecular weight in order to have complex viscosity comparable to SEBS.

Blending of PPO with the block copolymers resulted in lower values of all viscoelastic properties, with SIBS 103T showing the most pronounced decrease. A representative example is shown in Fig. 8 for blends containing 20 wt% block copolymer. It is worth noting that at the low thermoplastic rubber contents investigated here, all blends exhibit Newtonian plateaus, consistent with the TEM findings that PPO comprises the major phase. On the contrary, no Newtonian plateaus have been reported in SIBS-rich blends [10].

3.4. Mechanical properties

3.4.1. Dynamic mechanical thermal analysis (DMTA)

Fig. 9(a) presents the G' and loss tangent ($\tan\delta$) plots of the PPO/SIBS 103T blends at various compositions. The drop in G', and the peak in $\tan\delta$ around 220 °C are attributed to the glass transition of the hard PPO-rich phase. In the case of the 80/20 (w/w) blend, the modulus decrease in the temperature range of 25–200 °C is accompanied by a significant increase in the loss tangent ($\tan\delta$). These substantial changes

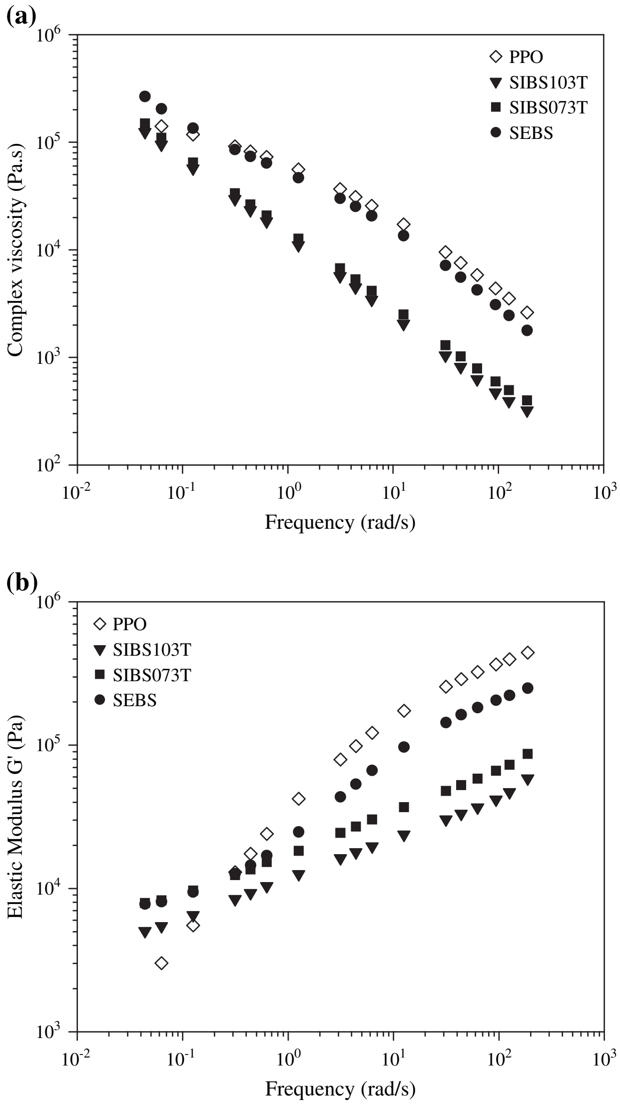

Fig. 7. (a) Complex viscosity of pure components at 240 °C. (b) Elastic modulus of pure components at 240 °C.

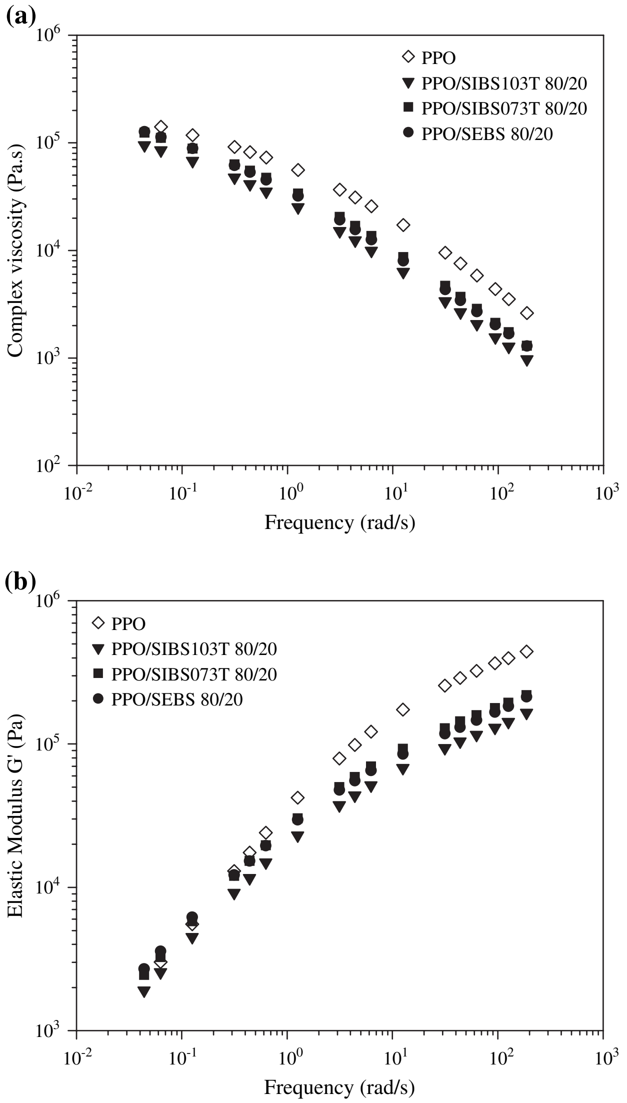

Fig. 8. (a) Complex viscosity for blends containing 20 wt% block copolymer at 240 °C. (b) Elastic moduli of blends containing 20 wt% block copolymer at 240 °C.

are most likely due to the presence of a co-continuous morphology, as seen by TEM (see also Fig. 3). Similar trends were observed in the PPO/SIBS 073T and PPO/SEBS blends and are attributed to the reduction in the stiffness of PPO upon incorporation of the soft block, and the ensuing increase in damping properties. For these materials the glass transition temperature did not show any prominent shifts, indicating little or no incorporation of the PSt segments of the block copolymers into the PPO phase. However, the PPO/SBS blends exhibit considerable shifts in the glass transition temperature toward lower temperatures (223 °C for pure PPO and 211 °C for PPO/SBS 80/20 see Fig. 9(b)), indicating strong incorporation of the PSt phases of the SBS block copolymers into the PPO. The T_g depression trends obtained from DMTA are similar to those obtained by DSC measurements. It is worth noting that PPO/SBS blends had similar elastic moduli, irrespective of composition, in the 100–200 °C range, and their stiffness was generally higher than that of the other blends, possibly because of the improved miscibility in the hard phase, as explained previously.

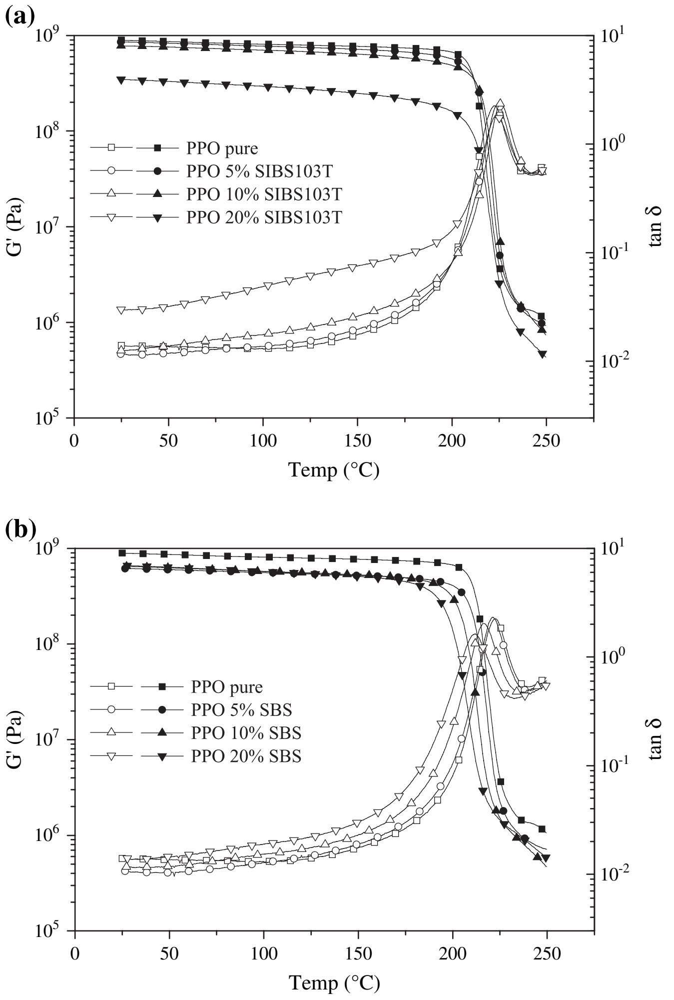

Fig. 9. (a) Storage modulus G' and tan δ versus temperature for various PPO/SIBS (103T) blends. Compositions are as indicated in the figure. (b) Storage modulus G' and tan δ versus temperature for various PPO/SBS blends.

3.4.2. Tensile and impact properties

Tensile strength decreased as the amount of block copolymers increased in the blends (Fig. 10), which was anticipated since block copolymers have substantially lower tensile strength than the pure PPO. SBS caused moderate decreases, whereas substantial decreases were noted for all other blends at high block copolymer contents. At 20% block content, the PPO/SIBS blends showed ~20 MPa ultimate strength. The PPO/SBS blends exhibited almost a linear increase of elongation from 5 to 20% with increasing SBS fraction in the blends. Increase in elongation to 15% was also noted for the blends containing SEBS, whereas no notable improvement was seen when the two SIBS copolymers were used. In comparison, commercial PPO–PSt blends with about 20 wt% PSt have tensile strength and elongation in the range of 60–90 MPa and 15–25%. For solution blends of PPO with 20 wt% SIBS, Asthana and Kennedy reported 10 MPa ultimate tensile

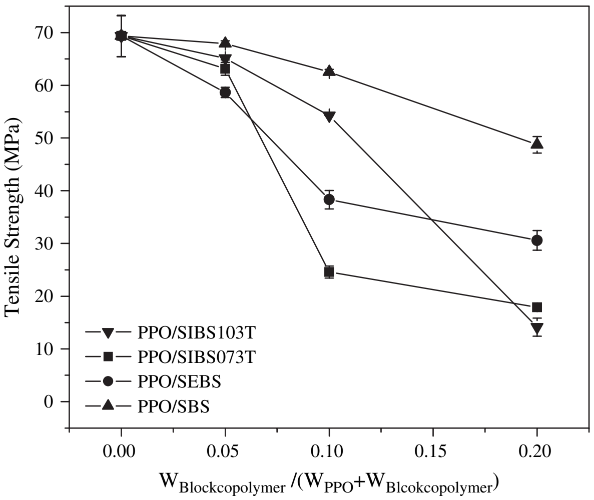

Fig. 10. The relationship between tensile strength and composition in PPO/block copolymers blends. Lines are drawn to guide the eye.

strength with 150% elongation, indicating the presence of a co-continuous rubber phase [10].

The impact strength of the blends investigated here was in the range of 1−3 kJ/m^2, similar to that of commercial PPO—PSt blends. Comparison of DMTA, tensile and impact properties reveals that out of the two SIBS block copolymers, SIBS 103T, which had higher PSt content, higher PSt block molecular weight and higher molecular weight overall, with broad molecular weight distribution and a branched structure, provided a better balance for toughness and stiffness.

4. Conclusions

Comparison of the effect of thermoplastic rubbers on PPO studied in this work revealed that PPO/SEBS blends have the most pronounced phase-separated morphology with larger rubbery domains. Out of the two new PIB-based thermoplastic rubbers investigated, SIBS 103T showed some degree of intermixing with PPO, leading to a better balance of processability and mechanical properties. The PPO/SIBS 103T 90/10 (w/w) blend had a good combination of impact strength and mechanical properties. SBS showed some miscibility with PPO, and had the least detrimental effect on mechanical properties. Although we found no improvement in terms of impact resistance in this study, the results pointed us to the right direction. We recently achieved impact strength in excess of 10 kJ/m^2, by the judicious selection of blending conditions: the details will be published separately.

Acknowledgements

Financial support by LANXESS Inc. (formerly Bayer Canada, Rubber Division) and NSERC is greatly appreciated. This work has been supported by the German Science Foundation (Deutsche Forschungsgemeinschaft DFG, SFB 481, project A10). The authors would like to thank Ms. W.Q. Wang for the rheological measurements.

References

[1] Hay AS. J Polym Sci Part A Polym Sci 1998;36:505.
[2] Wang X, Feng W, Li H, Ruckenstein E. Polymer 2002;43:37.
[3] Tucker PS, Barlow JW, Paul DR. Macromolecules 1988;21:1678.
[4] Mazard C, Benyahia L, Tassin J. Polym Int 2003;52:514.
[5] Dickie RA. In: Paul DR, Newman S, editors. Polymer blends, vol. 1. New York: Academic; 1978.
[6] Tucker PS, Barlow JW, Paul DR. Macromolecules 1988;21:2794.
[7] Chiu H-T, Hwung D-S. Eur Polym J 1994;30(10):1191.
[8] Paul DR. In: Holden G, Legge NR, Quirk R, Schroeder HE, editors. Thermoplastic elastomers. Munich: Hanser Publishers; 1996.
[9] Lach R, Grellmann W, Weidisch R, Altstädt V, Kirschnick T, Ott H, et al. J Appl Polym Sci 2000;78(11):2037.
[10] Asthana S, Kennedy JP. J Appl Polym Sci 2002;86:2866.
[11] Data refereed from Kaneka Research Lab.
[12] Puskas JP, Kaszas G. Rubber Chem Technol 1996;l69:3462.
[13] Jenkins AD. Advanced routes for polymer toughening. Elsevier Science Ltd; 2000.
[14] MacKnight WJ, Karasz FE, Fried JR. In: Paul DR, Newman S, editors. Polymer blends, vol. 1. New York: Academic; 1978 [chapter 5].
[15] Keskkula H, Paul DR, Young P, Stein RS. J Appl Polym Sci 1987;34:1861.
[16] Picchioni F, Casentini E, Passaglia E, Ruggeri G. J Appl Polym Sci 2003;88:2698.
[17] Brandrup J, Immergut EH, Grulke EA, editors. Polymer handbook. 4th ed. New York: Wiley; 1999.
[18] Datta S, Lohse DJ. Polymeric compatibilizers. New York: Hanser; 1996. p. 287.
[19] Wu S. Polym Eng Sci 1987;27(5):335.
[20] Favis BD, Willis JM. J Polym Sci Part B Polym Phys 1990;28:2259. 2000;41:163.
[21] Chung CI, Gale JC. J Polym Sci Polym Phys Ed 1976;14:1149.
[22] Tse MF, Wang H-C, Shaffer TD, McElrath KO, Modi MA, Krishnamoorti R. Polym Eng Sci 2000;40(10):2182.
[23] Gouinlock EV, Porter RS. Polym Eng Sci 1977;17:535.
[24] Antony P, Puskas JE, Kontopoulou M. Polym Eng Sci 2003;43(1):243.